Simulations of the spatial and temporal invariance in the spectra of gradual solar energetic particle events

ARTICLE *in* THE ASTROPHYSICAL JOURNAL · JUNE 2015

Impact Factor: 6.28 · DOI: 10.1088/0004-637X/806/2/252

2 AUTHORS:

Yang Wang
Chinese Academy of Sciences
7 PUBLICATIONS **12** CITATIONS
SEE PROFILE

Gang Qin
Chinese Academy of Sciences
55 PUBLICATIONS **926** CITATIONS
SEE PROFILE

SIMULATIONS OF THE SPATIAL AND TEMPORAL INVARIANCE IN THE SPECTRA OF GRADUAL SOLAR ENERGETIC PARTICLE EVENTS

Yang Wang[1] and Gang Qin[1]

ywang@spaceweather.ac.cn; gqin@spaceweather.ac.cn

Received _____; accepted _____

[1]State Key Laboratory of Space Weather, Center for Space Science and Applied Research, Chinese Academy of Sciences, Beijing 100190, China

ABSTRACT

The spatial and temporal invariance in the spectra of energetic particles in the gradual solar events is reproduced in the simulations. Based on a numerical solution of the focused transport equation, we obtain the intensity time profiles of solar energetic particles (SEPs) accelerated by an interplanetary shock in the three-dimensional interplanetary space. The shock is treated as a moving source of energetic particles with a distribution function. The time profiles of particle flux with different energies are calculated in the ecliptic at 1 AU. According to our model, we find that shock acceleration strength, parallel diffusion and adiabatic cooling are the main factors in forming the spatial invariance in SEP spectra, and perpendicular diffusion is a secondary factor. In addition, the temporal invariance in SEP spectra is mainly due to the effect of adiabatic cooling. Furthermore, a spectra invariant region, which agrees with observations but is different than the one suggested by Reames and co-workers, is proposed based on our simulations.

Subject headings: Sun: activity — Sun: coronal mass ejections (CMEs) — Sun: particle emission

1. INTRODUCTION

Solar energetic particle (SEP) events can roughly be divided into two categories: impulsive events and gradual events (Reames 1995, 1999). The impulsive events, with the characteristics of low intensity and short duration, are produced by solar flares. Gradual events, usually lasting longer and having high intensity, are related to the shocks driven by interplanetary coronal mass ejections (ICMEs). Lario et al. (2006) investigated the radial and longitudinal dependence of $4-13$ and $27-37$ MeV proton peak intensities and fluences measured within 1 AU. They found the peak intensities and fluences of SEP events can be approximated by $j = j_0 r^{-\alpha} \exp\left[-k(\phi - \phi_0)^2\right]$, where j is either the peak intensity or the fluence, r is the radial distance of the spacecraft, ϕ is the longitudinal angular distance between the footpoint of the observer's field line and the region of the SEP source, and ϕ_0 is the centroid of the distributions. Furthermore, the radial dependence of peak intensities and fluences of SEP events have been simulated with a focused-diffusion transport equation (Lario et al. 2007).

Generally, there are two major approaches to modeling SEP acceleration by CME driven shocks: some authors (Heras et al. 1992, 1995; Kallenrode & Wibberenz 1997; Lario et al. 1998; Kallenrode 2001; Ng et al. 2003; Wang et al. 2012; Qin et al. 2013) adopted a "black box" model to treat the shock as a moving source, and SEPs are injected at the shock with an assumed injection strength, while a few other studies include the acceleration of SEPs by shocks (Lee 1983; Gordon et al. 1999; Zank et al. 2000; Li et al. 2003; Rice et al. 2003; Sokolov et al. 2004; Li et al. 2005; Kóta et al. 2005; Tylka & Lee 2006; Zuo et al. 2011; Zuo et al. 2013). In these models, three important effects of acceleration and propagation mechanisms have been involved. The first effect is the acceleration process by the CME-driven shock. Zank et al. (2000) modeled the evolution of a CME-driven shock based on an "onion shell" model, and this model has been furtherly developed in a number of papers (Li et al. 2003; Rice et al. 2003; Li et al. 2005). They used a magnetohydrodynamics (MHD) code to describe the evolution of the CME-driven shock

in the interplanetary space, and wave excitation by streaming energetic particles produced at shock is included. Based on the model, the simulation results can successfully explain the SEP fluxes and spectra in some multi-spacecraft observed events (Verkhoglyadova et al. 2009, 2010). The second effect is energetic particles to interact with Alfv́en wave self-consistently. Ng et al. (2003, 2012) presented a model of particle transport including streaming proton-generated Alfv́en waves, and the amplification of the Alfv́en waves is determined by the anisotropy of particles. The particle diffusion coefficients can be calculated from wave intensity and wave growth rates. Their simulation results show a good agreement with the observed spectral slope and abundance ratios of heavy ions. The third effect is the realistic geometry of CME and its shock (Sokolov et al. 2004; Kóta et al. 2005). Sokolov et al. (2004) modeled particle acceleration and transport as CME driven shock wave propagating from 4 to 30 solar radius from the Sun. The realistic structures of CME and its shock are derived from a numerical solution of a fully three-dimensional MHD model. Their simulation results demonstrate that the diffusive shock acceleration theory can account for the increase of hundreds of MeV protons during the early stages of CME driven shock.

Solar energetic particle events measured by multi-spacecraft help us to understand the processes of particle acceleration and transport in the heliosphere. In some gradual events, the SEP fluxes measured by widely separated spacecraft present similar intensities within a small $\sim 2-3$ factor in different latitudes, longitudes or radius (Reames et al. 1997; Reames 2010, 2013; McKibben et al. 2001b; Maclennan et al. 2001; Lario et al. 2003; Tan et al. 2009). This phenomenon was firstly proposed by McKibben (1972), and was named “reservoir” by Roelof et al. (1992). In order to interpret the reservoir phenomenon, McKibben (1972) and McKibben et al. (2001b) involved an effective perpendicular diffusion to reduce the spatial gradients of flux, while Roelof et al. (1992) suggested a diffusion barrier produced by ICMEs or shocks. The magnitude of magnetic field increases at the outer boundary of reservoirs, so that SEPs could be contained in the reservoirs for a long time. Furthermore, the interplanetary magnetic field (IMF) has been disturbed by ICMEs, SEPs could be redistributed. Reames et al. (1996) shows

that, in some gradual SEP events, the spectra are invariant both in space and time. This discovery extended the original work of McKibben (1972). In Reames et al. (1996), they considered an expanding magnetic bottle of quasi-trapped particles between an ICME driven shock and the Sun. As the magnetic bottle expanding, the SEP fluxes gradually decrease as a result of parallel diffusion and adiabatic cooling. In this sense, the magnetic bottle plays a pivotal role in the decay phase of SEP event.

In principle, the disturbances in the magnetic field caused by ICMEs can help the particles redistribute in space. However, the reservoir phenomenon cannot be simply explained as a result of the disturbances of IMF caused by ICMEs. Firstly, in the redistribution process in Reames et al. (1996) and Reames (2013), no explicit transport mechanism can reduce latitudinal, longitudinal, and radial gradients of SEP fluxes besides perpendicular diffusion. Secondly, in some SEP events, ICMEs are not directly observed by the spacecraft, the reservoir phenomenon is also observed (McKibben et al. 2001a). Thirdly, in Reames (1999), when the observer is located at the eastern of the shock, the onset time of temporal invariance in the SEP spectra is earlier than the shock arrival time. These results are not consistent with that of an expanding magnetic bottle.

The effect of perpendicular diffusion is important in the SEP fluxes especially when the observer is disconnected from the shock by IMF. During the time period March 1, 1979 to March 11, 1979, a gradual SEP event has been detected by *Helios* 1, *Helios* 2, and *IMP* 8. The three spacecraft are located in the ecliptic near 1 AU, but at different longitudes. In the decay phase of this SEP event, the reservoir phenomenon appeared (Reames et al. 1997; Reames 1999, 2010, 2013). In this event, the in-situ observation shows that an ICME was detected by *Helios* 1, but not by *Helios* 2 and *IMP* 8. And the interplanetary shock was only observed by *Helios* 1 and 2, but not by *IMP* 8 (Lario et al. 2006; Reames 2010). According to the location of the three spacecraft, if the ICME was located behind the center of the shock front, then *Helios* 1 was located near to the center of shock, and *Helios* 2 and *IMP* 8 were located at the West frank of the shock. However,

the onset time of SEP fluxes observed by three spacecraft was very close. How could SEPs be detected by *IMP* 8 before it was connected to the shock by IMF? One possible answer is the effect of perpendicular diffusion which also possibly works in forming the reservoir phenomenon.

However, perpendicular diffusion has been always a difficult problem for several decades. Observation results show various levels of perpendicular diffusion coefficients for different SEP events. For example, 'dropout' phenomenon in the impulsive SEP event (Mazur et al. 2000) usually show reduced perpendicular diffusion, in order to reproduce the 'dropout' phenomenon in simulations, perpendicular diffusion coefficient $\kappa_\perp$ should be several order magnitude smaller than parallel one $\kappa_\parallel$ (Giacalone et al. 2000; Guo & Giacalone 2014; Dröge et al. 2010; Wang et al. 2014). On the other hand, for some events, observation results show that the perpendicular diffusion coefficients could be comparable to the parallel ones (Dwyer et al. 1997; Zhang et al. 2003; Dresing et al. 2012). In order to understand diffusion, many efforts were made theoretically. By assuming energetic particles' perpendicular and parallel diffusion do not interaction, Jokipii (1966) developed the quasi-linear theory (QLT). According to QLT, perpendicular diffusion coefficient is usually much smaller than the parallel one. However, it is found that interaction between parallel and perpendicular diffusion is important in theory (Kóta & Jokipii 2000) and in simulations (Qin et al. 2002b,a), so the non-linear guiding center (NLGC) theory (Matthaeus et al. 2003) is developed to describe perpendicular diffusion with the influence of parallel diffusion, which agrees with simulations much better than QLT. In addition, simulations show different levels of perpendicular diffusion, e.g., in Qin & Shalchi (2012), the magnitude of $\kappa_\perp/\kappa_\parallel$ could be as large as 10^{-1} in some conditions, and as small as 10^{-4} in other conditions.

Recently, Qin et al. (2013) proposed that the shock acceleration strength makes important contributions to the reservoir phenomenon, particularly in low-energy SEPs. In their simulations, the reservoir phenomenon is reproduced under a variety of conditions of shock acceleration strength and perpendicular diffusion. In this paper, as a continuation of Qin et al. (2013), we study

the property of SEP spectra in the decay phase. We compute the time profiles of SEP flux which are accelerated by interplanetary shock. In section 2 we describe the SEP transport model and the shock model. In Section 3 we show the simulation results. In Section 4 we summary our results.

2. MODEL

In this work, we model the transport of SEPs following previous research(e.g., Qin et al. 2006; Zhang et al. 2009; Dröge et al. 2010; He et al. 2011; Zuo et al. 2011; Wang et al. 2012; Qin et al. 2013; Zuo et al. 2013; Wang et al. 2014). A three-dimensional focused transport equation is written as (Skilling 1971; Schlickeiser 2002; Qin et al. 2006; Zhang et al. 2009)

$$\begin{aligned}\frac{\partial f}{\partial t} &= \nabla\cdot(\boldsymbol{\kappa}_{\perp}\cdot\nabla f) - \left(v\mu\,\hat{\boldsymbol{b}} + \boldsymbol{V}^{sw}\right)\cdot\nabla f + \frac{\partial}{\partial\mu}\left(D_{\mu\mu}\frac{\partial f}{\partial\mu}\right)\\ &+p\left[\frac{1-\mu^2}{2}\left(\nabla\cdot\boldsymbol{V}^{sw} - \hat{\boldsymbol{b}}\,\hat{\boldsymbol{b}} : \nabla\boldsymbol{V}^{sw}\right) + \mu^2\,\hat{\boldsymbol{b}}\,\hat{\boldsymbol{b}} : \nabla\boldsymbol{V}^{sw}\right]\frac{\partial f}{\partial p}\\ &-\frac{1-\mu^2}{2}\left[-\frac{v}{L} + \mu\left(\nabla\cdot\boldsymbol{V}^{sw} - 3\,\hat{\boldsymbol{b}}\,\hat{\boldsymbol{b}} : \nabla\boldsymbol{V}^{sw}\right)\right]\frac{\partial f}{\partial\mu},\end{aligned} \tag{1}$$

where $f(\boldsymbol{x},\mu,p,t)$ is the gyrophase-averaged distribution function; $\boldsymbol{x}$ is the position in a non-rotating heliographic coordinate system; t is the time; μ, p, and v are the particle pitch-angle cosine, momentum, and speed, respectively, in the solar wind frame; $\hat{\boldsymbol{b}}$ is a unit vector along the local magnetic field; $\boldsymbol{V}^{sw} = V^{sw}\,\hat{\boldsymbol{r}}$ is the solar wind velocity; and L is the magnetic focusing length given by $L = \left(\hat{\boldsymbol{b}}\cdot\nabla lnB_0\right)^{-1}$ with B_0 being the magnitude of the background magnetic field. The IMF is set as the Parker field model, and the solar wind speed is 400 km/s. This equation includes many important particle transport effects such as particle streaming along the field line, adiabatic cooling in the expanding solar wind, magnetic focusing in the diverging IMF, and the diffusion coefficients parallel and perpendicular to the IMF.

The pitch angle diffusion coefficient model is set as (Beeck & Wibberenz 1986; Qin et al.

2005)

$$D_{\mu\mu} = D_0 \upsilon p^{q-2} \left\{ |\mu|^{q-1} + h \right\} \left(1 - \mu^2\right), \tag{2}$$

where the constant D_0 controls the magnetic field fluctuation level. The constant q is chosen as $5/3$ for a Kolmogorov spectrum type of the power spectra density of magnetic field turbulence in the inertial range. Furthermore, $h = 0.01$ is chosen for the non-linear effect of pitch-angle diffusion at $\mu = 0$ in the solar wind (Qin & Shalchi 2009, 2014).

The parallel mean free path (MFP) $\lambda_\parallel$ can be written as (Jokipii 1966; Hasselmann 1968; Earl 1974)

$$\lambda_\parallel = \frac{3\upsilon}{8} \int_{-1}^{+1} \frac{(1-\mu^2)^2}{D_{\mu\mu}} d\mu, \tag{3}$$

and the parallel diffusion coefficient $\kappa_\parallel$ can be written as $\kappa_\parallel = v\lambda_\parallel/3$.

The relation of the particle momentum and the perpendicular diffusion coefficient is set as (Potgieter & Moraal 1985; Zhang 1999)

$$\boldsymbol{\kappa}_\perp = \kappa_0 \left(\frac{v}{c}\right) \left(\frac{p}{1\ \mathrm{GeV}c^{-1}}\right)^\alpha \left(\frac{B_e}{B}\right) \left(\mathbf{I} - \hat{\mathbf{b}}\,\hat{\mathbf{b}}\right) \tag{4}$$

where B_e is magnetic field strength at the Earth, B is the magnetic field strength at the location of particle, p is particle momentum, and α is set to $1/3$. Different perpendicular diffusion coefficients could be obtained by altering κ_0. Note that we use this ad-hoc model for the purpose of simplicity, the parameters, e.g., α could be set as other values (Zhang 1999). However, the variation of these parameters would not qualitatively change the results in this paper. There are some more complete models that are developed to describe the particle diffusion in magnetic turbulence, such as the nonlinear guiding center theory (Matthaeus et al. 2003; Shalchi et al. 2004, 2010; Qin & Zhang 2014).

We use a time-backward Markov stochastic process method to solve the transport equation (1). The detail of method can be found in Zhang (1999) and Qin et al. (2006). The particle injection on the shock is specified by boundary values. The boundary condition is chosen as

following form (Kallenrode & Wibberenz 1997; Kallenrode 2001; Wang et al. 2012; Qin et al. 2013)

$$\begin{aligned} f_b(r,\theta,\varphi,p,t) &= a\cdot\delta(r-\upsilon_s t)\cdot S(r,\theta,\varphi,p)\cdot p^{-\gamma}\cdot\xi(\theta,\varphi) \\ S(r,\theta,\varphi,p) &= (\frac{r}{r_c})^{-\alpha(p)}\cdot\exp\left[-\frac{|\phi(\theta,\varphi)|}{\phi_c(p)}\right] \\ \xi(\theta,\varphi) &= \begin{cases} 1 & \text{if } |\phi(\theta,\varphi)|\le\phi_s \\ 0 & \text{otherwise,} \end{cases} \end{aligned} \tag{5}$$

where the particle are injected at $r = \upsilon_s t$, υ_s is shock speed. $\upsilon_s t = r_0 + n\cdot\Delta r$, with $n = 0, 1, 2\cdots n_0$. Δr is space interval between two 'fresh' injections, $r_0 = 0.05\ AU$ is inner boundary. r_c is set to 0.05. r is distance between sun and shock. ϕ is the angle between the center of shock and the point at the shock front where the particles injected. The shock acceleration strength is set as S for specifying the particles ejection. It changes with a power law in radial distance and exponential towards the flank of shock. ξ determines the spatial scale of shock front. ϕ_s is the half width of the shock.

3. RESULTS

The parameters used are listed in table 1, unless otherwise stated. Note that the IMF is set as Parker spiral, and the disturbances of IMF behind the shock are ignored. The particle energy channels are chosen as 5 MeV, 10 MeV, 20 MeV, 40 MeV and 80 MeV. The parallel mean free path depends on the momentum $\lambda_\parallel \sim p^{1/3}$. According to Qin et al. (2013), the $\kappa_\perp/\kappa_\parallel$ is set as 0.1 in the ecliptic at 1 AU. Because the shock acceleration efficient decreases as the particle energy increasing, the acceleration strength parameters also change with the momentum: $\alpha \sim p^{0.3}$, $\phi_c \sim p^{-0.3}$. The observers are located in the ecliptic at 1 AU.

3.1. Temporal Invariance in the Spectra

In Figure 1 and 2, we plotted the fluxes of different energy channels in the cases with and without adiabatic cooling. In order to check the temporal properties of SEP spectra in the decay phase, we normalize different energy fluxes, so that the fluxes have similar values soon after all of them have reached peaks. The panels show the normalized fluxes observed in the ecliptic at 1 AU, but at different longitudes E60, E20, W20 and W60. The notations E60, E20, W20, W60 are short for East 60°, East 20°, West 20° and West 60°, respectively. East/West means the location of the observer is east/west relative to the center of shock. The vertical lines indicate the shocks passage of the observers.

In Figure 1, the adiabatic cooling effect is included in SEP propagation process. In the decay phase of SEP events, shock acceleration strength, adiabatic cooling, parallel diffusion, and perpendicular diffusion are the major factors to influence the flux behavior. In the four panels, the fluxes at all energies follow a similar trend, then the fluxes scatter slowly as time goes by. This is called temporal invariance in the spectra of gradual SEP event. In the E60 event, the fluxes at all energies start to follow a similar trend about one day before the shock passage of 1 AU. In other words, the onset time of the temporal invariance is earlier than the time of the shock passage of the observer. In the E20 and W20 events, however, the onset time of temporal invariance is close to the shock passage of the observers. In the W60 event, furthermore, the temporal invariance starts the latest, and actually it starts two days latter than the shock arrival.

In Figure 2, the adiabatic cooling is not included in the SEP propagation process. Without adiabatic cooling, shock acceleration strength, parallel and perpendicular diffusion are the major factors in the decay phase. Due to the different diffusion coefficients and shock acceleration strength for different energy particles, the fluxes decay with different ratios consequently. With higher energies, the fluxes decay much faster. In these cases, the temporal invariance does not exist in the decay phase.

Comparing Figure 1 and Figure 2, the fluxes decrease much faster with adiabatic cooling. Because of adiabatic energy loss, particles have less energy when they are observed than that when they are released in the sources. In addition, since the source spectrum index is negative, the fluxes are lower with higher energies, so that the adiabatic cooling effect makes the SEP flux decreasing as time passes by. To sum up, the temporal invariance in the spectra results from the adiabatic cooling effect.

3.2. Spatial Invariance in the Spectra

In Figure 3, the SEP fluxes are shown for three observers located at different longitudes, E20, W20, and W60. The upper panel shows the 5 MeV proton fluxes observed by the observers. We set two typical time intervals, interval *A* from 1.3 days to 1.5 days in rising phase and interval *B* from 6.9 days to 7.1 days in decay phase. In order to study the spatial variance in different phases, in lower left and right panels of Figure 3, we plot the energy spectra observed in different longitudes in interval *A* and interval *B*, respectively. During the interval *A*, the spectra are different among the three observers. However, during the interval *B*, spectra are almost the same among the three observers. This phenomenon, which is named spatial invariance in the spectra by Reames et al. (1997), results from the reservoir effect in different energy channels.

Because the shock is a moving source in the interplanetary space, the peak intensity of SEP flux is mainly determined by the shock acceleration strength and parallel MFP. In upper panel of Figure 3, at the peak time of flux for W20 (W60), the flux for W20 (W60) is close to that for E20. Furthermore, the SEP fluxes decay in a similar ratio because of the effect of adiabatic cooling. At the same time, the latitudinal gradient in the SEP fluxes is further reduced because of the effect of perpendicular diffusion. However, in other simulations with different shock acceleration strength and parallel MFP (not shown here), if at the peak time of flux for W20 (W60), the flux for W20 (W60) is significantly different than that for E20, the reservoir phenomenon can not form

in normal diffusion coefficients. As a result, shock acceleration strength, parallel diffusion, and adiabatic cooling are the main factors in forming the reservoir phenomenon, and perpendicular diffusion is a secondary factor.

3.3. Invariant Spectra Region

There are some important characteristics in the invariant spectra region from our simulations (Figure 1). If the observer is located at the eastern flank of the shock, the onset time of invariant spectra is earlier than the shock arrival. But if the observer is located near the central flank of shock, the spectra invariance begins approximately at the shock passages. Finally, if the observer is located at the western flank of shock, the onset time of invariant spectra are much later than the shock arrivals. From these results, we can better understand the invariant spectra region.

Figure 4 shows the invariant spectra region. In the picture, the green line is plotted by Reames et al. (1997), and the red line is new in this work. According to Reames et al. (1997), the left side of the green line is the invariant spectra region, with the assumption that particles are quasi-trapped in the region behind the ICME, and the SEP fluxes gradually decrease as a result of parallel diffusion and adiabatic deceleration mechanisms, and in addition, there are also some leakage of energetic particles from ICME to eastern side of the upstream shock. In this sense, ICMEs play the pivotal role in the decay phase of fluxes. As a result, the invariant spectra region is determined by ICMEs' propagation path plus some eastern side of upstream region. However, we suppose the invariant spectra region could be in the left side of the red line instead. In our simulations, ICME is not included, but in the propagation process perpendicular diffusion is included to reduce the spatial gradient in the fluxes, and adiabatic cooling is included to reduce the temporal variance. As the simulation results showed above, the spectra spatial and temporal invariance could result from the effects of shock acceleration strength, adiabatic cooling, and perpendicular diffusion. In this sense, it is possible that the invariant spectra region is not confined

by the ICMEs' propagation path. Instead, the invariant spectra region could be confined by the interplanetary shock, but the region expands faster (slower) than the shock at the eastern (western) flank, respectively.

4. DISCUSSION AND CONCLUSIONS

We have studied interplanetary shock accelerated SEPs propagation in three-dimensional IMF. The spectra observed by different observers are calculated, and the spatial and temporal invariance in the spectra are reproduced in the simulations. The following are our major findings.

The adiabatic cooling effect is the key factor for forming temporal invariance in the spectra. By including the adiabatic cooling, for different energy channels, the flux decay ratios are almost the same. The temporal invariance results from the fact that all energy particles decay as the same ratios because of adiabatic cooling effect. At the eastern flank of the shock, the onset time of the spectra invariance is earlier than the shock arrival. For the central cases, however, the onset time of the spectra invariance is close to the time of shock arrival. At the western flank of the shock, finally, the onset time of the spectra invariance is later than shock arrival. In addition, the fluxes decay much faster in the cases with adiabatic cooling. Without adiabatic cooling, the decay phase of SEP fluxes are dominated by shock acceleration strength, parallel diffusion, and perpendicular diffusion, which are all varying with particles' energies. Therefore, the temporal invariance does not exist without adiabatic cooling.

Shock acceleration strength, parallel diffusion, adiabatic cooling, and perpendicular diffusion are four important factors in forming the spatial invariance, which is in reservoir phenomenon in different energy channels. Shock acceleration strength parameters α and ϕ_c are set to 2 and 15° for 5 MeV protons in our simulations, respectively. And these parameters also change with the momentum: $\alpha \sim p^{0.3}$, $\phi_c \sim p^{-0.3}$, because the shock acceleration strength decreases with higher

energy particles. Among the four factors, shock acceleration strength, parallel diffusion, and adiabatic cooling are the main factors in forming the reservoir phenomenon, and perpendicular diffusion is a secondary one. This conclusion is derived based on our simulations, and it is also consistent with the observations. In Reames et al. (1997) and Reames (2013), a gradual SEP event was detected by *Helios* 1, *Helios* 2, and *IMP* 8 during March 1, 1979 to March 11, 1979. In this event, the reservoir phenomenon appeared, and the onset time of SEPs observed by different spacecraft are very close because of the effect of perpendicular diffusion. At the peak time of flux observed by *Helios* 2 (*IMP* 8), the flux observed by *Helios* 2 (*IMP* 8) is close to that observed by *Helios* 1. The importance of the peak intensity of SEP flux observed by *Helios* 2 and *IMP* 8 in forming the reservoir phenomenon is also noticed by Reames (2013), however, the reservoir phenomenon is explained as a result of the disturbance of IMF caused ICMEs. In our model, the peak of flux is mainly determined by shock acceleration strength and parallel diffusion. Furthermore, the SEP fluxes decay as a similar ratio because of the effect of adiabatic cooling. At the same time, the latitudinal gradient in the SEP fluxes is further reduced because of the effect of perpendicular diffusion. Finally, according to our model, the reservoir phenomenon appeared in this SEP event with the effects of shock acceleration strength, parallel diffusion, adiabatic cooling, and perpendicular diffusion. Observationally, shock acceleration strength, diffusion coefficients, and adiabatic cooling change significantly in different SEP events (Kallenrode 1996, 1997). As a result, the reservoir phenomenon can only form in some gradual SEP events with those controlling effect parameters in appropriate values.

Based on our simulations, a new invariant region is proposed. The new region is different from the one proposed by Reames et al. (1997). There are two important characteristics in our new region. First, if the observer is located at the eastern (western) flank of the shock, the onset time of temporal invariant in the spectra is earlier (later) than the shock arrival, respectively. Second, the spatial invariance in the spectra can also be formed without ICMEs. These two characteristics are supported by observations, but are difficult to be explained in the previous model Reames et al.

(1997).

In our model, we ignore the disturbance of the IMF caused by ICME for the simplicity. In principle, the disturbance in the magnetic field can help particles redistribute in space. In future work, we intend to include a realistic three-dimensional ICME shock, so that the SEP acceleration and transport in the heliosphere can be investigated more precisely.

The authors thank the anonymous referee for valuable comments. We are partly supported by grants NNSFC 41374177, NNSFC 41125016, and NNSFC 41304135, the CMA grant GYHY201106011, and the Specialized Research Fund for State Key Laboratories of China. The computations were performed by Numerical Forecast Modeling R&D and VR System of State Key Laboratory of Space Weather and Special HPC work stand of Chinese Meridian Project.

REFERENCES

Beeck, J., & Wibberenz, G. 1986, ApJ, 311, 437

Dresing, N., Gómez-Herrero, R., Klassen, A., Heber, B., Kartavykh, Y., & Dröge, W. 2012, Sol. Phys., 281, 281

Dröge, W., Kartavykh, Y. Y., Klecker, B., & Kovaltsov, G. A. 2010, ApJ, 709, 912

Dwyer, J. R., Mason, G. M., Mazur, J. E., Jokipii, J. R., von Rosenvinge, T. T., & Lepping, R. P. 1997, ApJ, 490, L115+

Earl, J. 1974, The Astrophysical Journal, 193, 231

Giacalone, J., Jokipii, J., & Mazur, J. 2000, The Astrophysical Journal Letters, 532, L75

Gordon, B. E., Lee, M. A., Möbius, E., & Trattner, K. J. 1999, J. Geophys. Res., 104, 28263

Guo, F., & Giacalone, J. 2014, The Astrophysical Journal, 780, 16

Hasselmann, K. 1968, Z. Geophys., 34, 353

He, H.-Q., Qin, G., & Zhang, M. 2011, The Astrophysical Journal, 734, 74

Heras, A. M., Sanahuja, B., Lario, D., Smith, Z. K., Detman, T., & Dryer, M. 1995, ApJ, 445, 497

Heras, A. M., Sanahuja, B., Smith, Z. K., Detman, T., & Dryer, M. 1992, ApJ, 391, 359

Jokipii, J. R. 1966, ApJ, 146, 480

Kallenrode, M. 1996, J. Geophys. Res., 101, 24393

—. 1997, J. Geophys. Res., 102, 22347

—. 2001, J. Geophys. Res., 106, 24989

Kallenrode, M., & Wibberenz, G. 1997, J. Geophys. Res., 102, 22311

Kóta, J., & Jokipii, J. R. 2000, ApJ, 531, 1067

Kóta, J., Manchester, W. B., Jokipii, J. R., de Zeeuw, D. L., & Gombosi, T. I. 2005, in American Institute of Physics Conference Series, Vol. 781, The Physics of Collisionless Shocks: 4th Annual IGPP International Astrophysics Conference, ed. G. Li, G. P. Zank, & C. T. Russell, 201–206

Lario, D., Aran, A., Agueda, N., & Sanahuja, B. 2007, Advances in Space Research, 40, 289

Lario, D., Kallenrode, M.-B., Decker, R. B., Roelof, E. C., Krimigis, S. M., Aran, A., & Sanahuja, B. 2006, ApJ, 653, 1531

Lario, D., Roelof, E. C., Decker, R. B., & Reisenfeld, D. B. 2003, Advances in Space Research, 32, 579

Lario, D., Sanahuja, B., & Heras, A. M. 1998, ApJ, 509, 415

Lee, M. A. 1983, J. Geophys. Res., 88, 6109

Li, G., Zank, G. P., & Rice, W. K. M. 2003, Journal of Geophysical Research (Space Physics), 108, 1082

—. 2005, Journal of Geophysical Research (Space Physics), 110, 6104

Maclennan, C. G., Lanzerotti, L. J., & Roelof, E. C. 2001, AGU Spring Meeting Abstracts, 31

Matthaeus, W. H., Qin, G., Bieber, J. W., & Zank, G. P. 2003, ApJ, 590, L53

Mazur, J., Mason, G., Dwyer, J., Giacalone, J., Jokipii, J., & Stone, E. 2000, The Astrophysical Journal Letters, 532, L79

McKibben, R. B. 1972, J. Geophys. Res., 77, 3957

McKibben, R. B., Lopate, C., & Zhang, M. 2001a, Space Sci. Rev., 97, 257

McKibben, R. B., et al. 2001b, in International Cosmic Ray Conference, Vol. 8, International Cosmic Ray Conference, 3281–+

Ng, C. K., Reames, D. V., & Tylka, A. J. 2003, ApJ, 591, 461

Ng, C. K., Reames, D. V., & Tylka, A. J. 2012, in American Institute of Physics Conference Series, Vol. 1436, American Institute of Physics Conference Series, ed. J. Heerikhuisen, G. Li, N. Pogorelov, & G. Zank, 212–218

Potgieter, M. S., & Moraal, H. 1985, ApJ, 294, 425

Qin, G., Matthaeus, W. H., & Bieber, J. W. 2002a, ApJ, 578, L117

—. 2002b, Geophys. Res. Lett., 29, 1048

Qin, G., & Shalchi, A. 2009, The Astrophysical Journal, 707, 61

Qin, G., & Shalchi, A. 2012, Advances in Space Research, 49, 1643

Qin, G., & Shalchi, A. 2014, Physics of Plasmas (1994-present), 21, 042906

Qin, G., Wang, Y., Zhang, M., & Dalla, S. 2013, The Astrophysical Journal, 766, 74

Qin, G., & Zhang, L.-H. 2014, The Astrophysical Journal, 787, 12

Qin, G., Zhang, M., Dwyer, J., Rassoul, H., & Mason, G. 2005, The Astrophysical Journal, 627, 562

Qin, G., Zhang, M., & Dwyer, J. R. 2006, Journal of Geophysical Research (Space Physics), 111, 8101

Reames, D. V. 1995, Reviews of Geophysics Supplement, 33, 585

—. 1999, Space Sci. Rev., 90, 413

—. 2010, Sol. Phys., 265, 187

—. 2013, Space Sci. Rev., 175, 53

Reames, D. V., Barbier, L. M., & Ng, C. K. 1996, ApJ, 466, 473

Reames, D. V., Kahler, S. W., & Ng, C. K. 1997, ApJ, 491, 414

Rice, W. K. M., Zank, G. P., & Li, G. 2003, Journal of Geophysical Research (Space Physics), 108, 1369

Roelof, E. C., Gold, R. E., Simnett, G. M., Tappin, S. J., Armstrong, T. P., & Lanzerotti, L. J. 1992, Geophys. Res. Lett., 19, 1243

Schlickeiser, R. 2002, Cosmic Ray Astrophysics, ed. Schlickeiser, R.

Shalchi, A., Bieber, J. W., Matthaeus, W. H., & Qin, G. 2004, ApJ, 616, 617

Shalchi, A., Li, G., & Zank, G. P. 2010, Ap&SS, 325, 99

Skilling, J. 1971, ApJ, 170, 265

Sokolov, I. V., Roussev, I. I., Gombosi, T. I., Lee, M. A., Kóta, J., Forbes, T. G., Manchester, W. B., & Sakai, J. I. 2004, ApJ, 616, L171

Tan, L. C., Reames, D. V., Ng, C. K., Saloniemi, O., & Wang, L. 2009, ApJ, 701, 1753

Tylka, A. J., & Lee, M. A. 2006, ApJ, 646, 1319

Verkhoglyadova, O. P., Li, G., Zank, G. P., Hu, Q., & Mewaldt, R. A. 2009, ApJ, 693, 894

Verkhoglyadova, O. P., et al. 2010, Journal of Geophysical Research (Space Physics), 115, 12103

Wang, Y., Qin, G., & Zhang, M. 2012, The Astrophysical Journal, 752, 37

380 Wang, Y., Qin, G., Zhang, M., & Dalla, S. 2014, ApJ, 789, 157

381 Zank, G. P., Rice, W. K. M., & Wu, C. C. 2000, J. Geophys. Res., 105, 25079

382 Zhang, M. 1999, ApJ, 513, 409

383 Zhang, M., Jokipii, J. R., & McKibben, R. B. 2003, ApJ, 595, 493

384 Zhang, M., Qin, G., & Rassoul, H. 2009, ApJ, 692, 109

385 Zuo, P., Zhang, M., Gamayunov, K., Rassoul, H., & Luo, X. 2011, ApJ, 738, 168

386 Zuo, P., Zhang, M., & Rassoul, H. K. 2013, The Astrophysical Journal, 767, 6

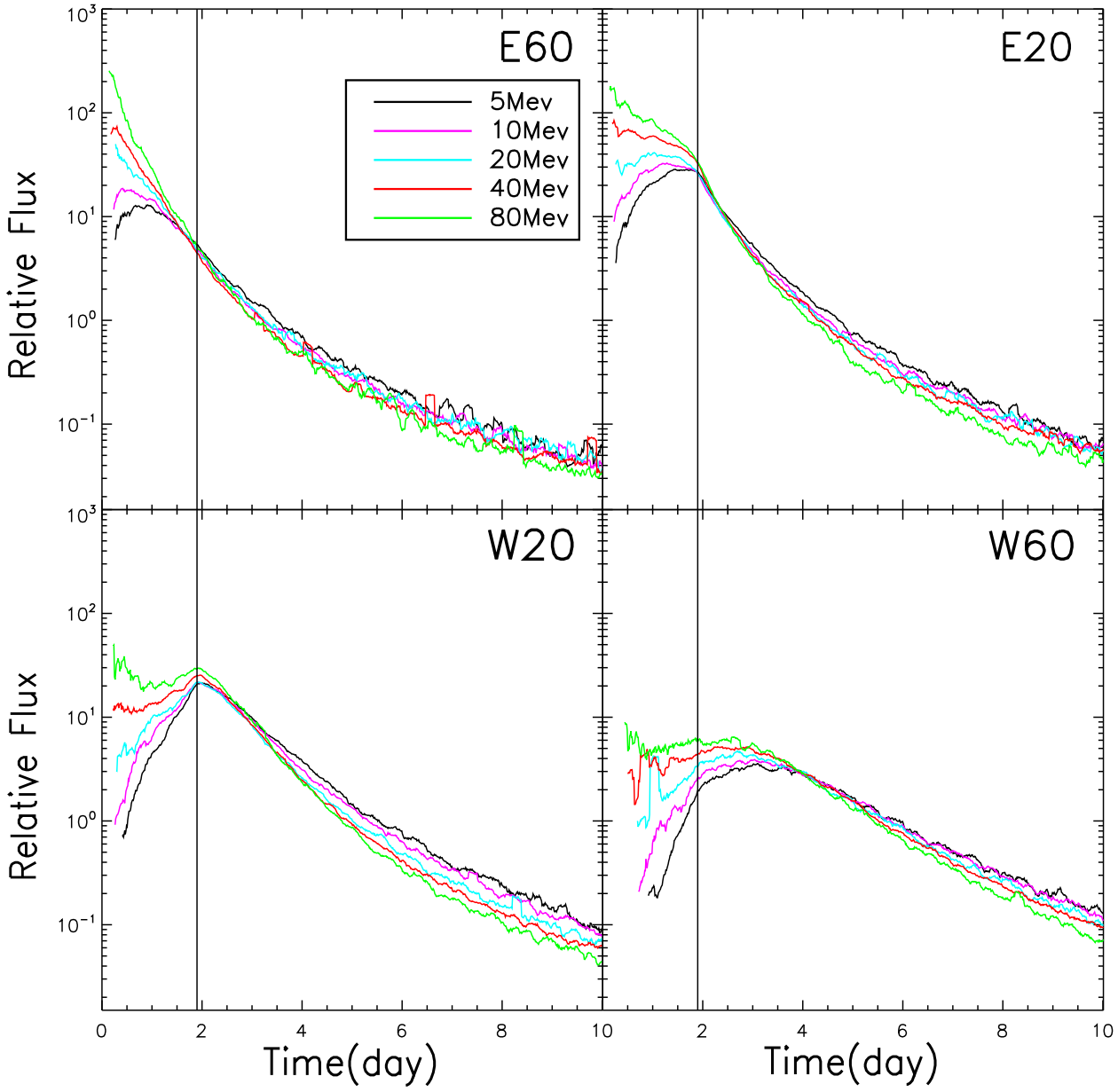

Fig. 1.— Comparison of different energy protons observed by observers in the 1 AU ecliptic at different longitudes. The fluxes are normalized so their values are similar after all of them reach peaks. The vertical lines indicate the shocks passage of 1 AU. The adiabatic cooling is included in simulations.

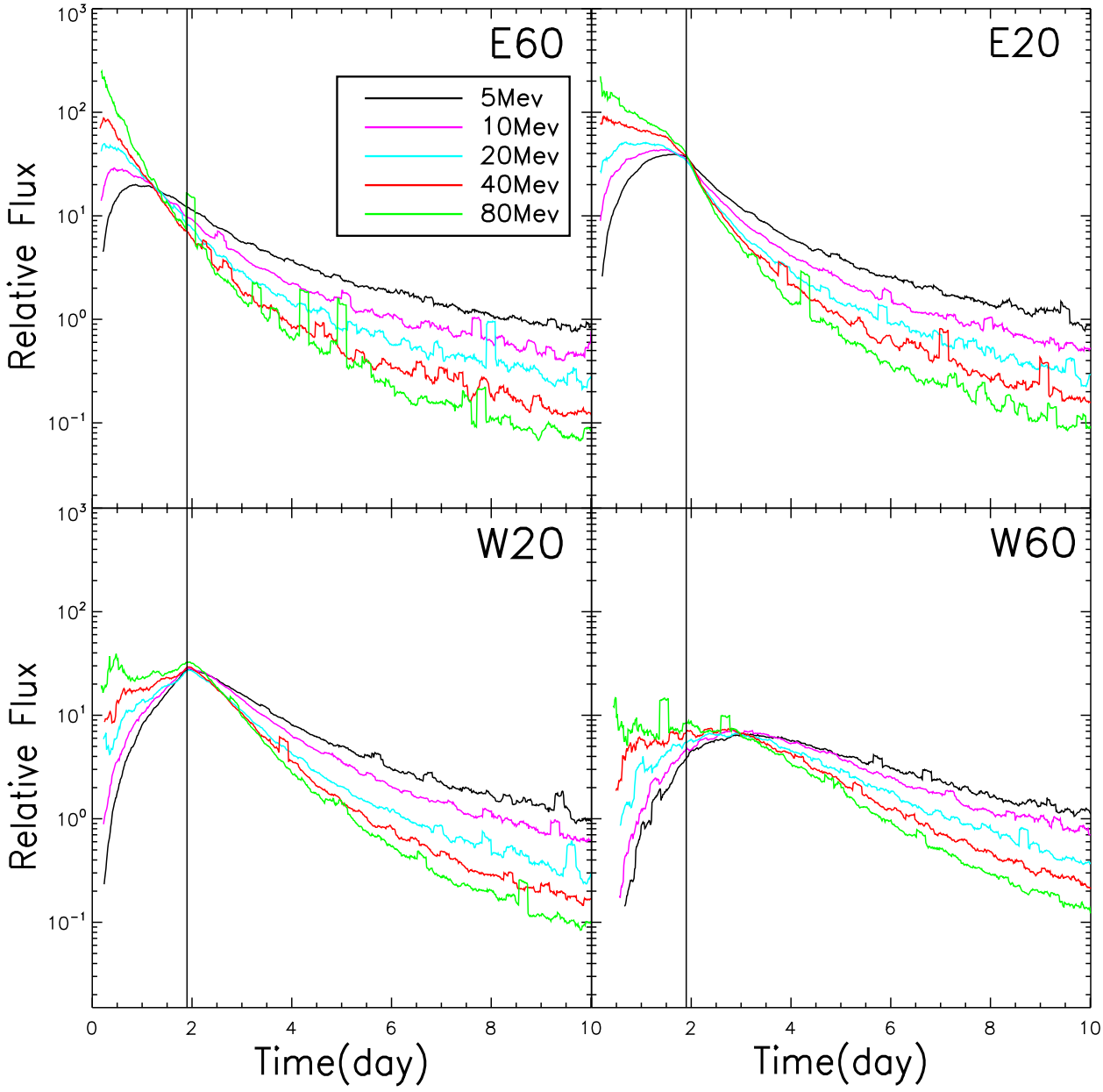

Fig. 2.— Same as 1 except that the adiabatic cooling is not included.

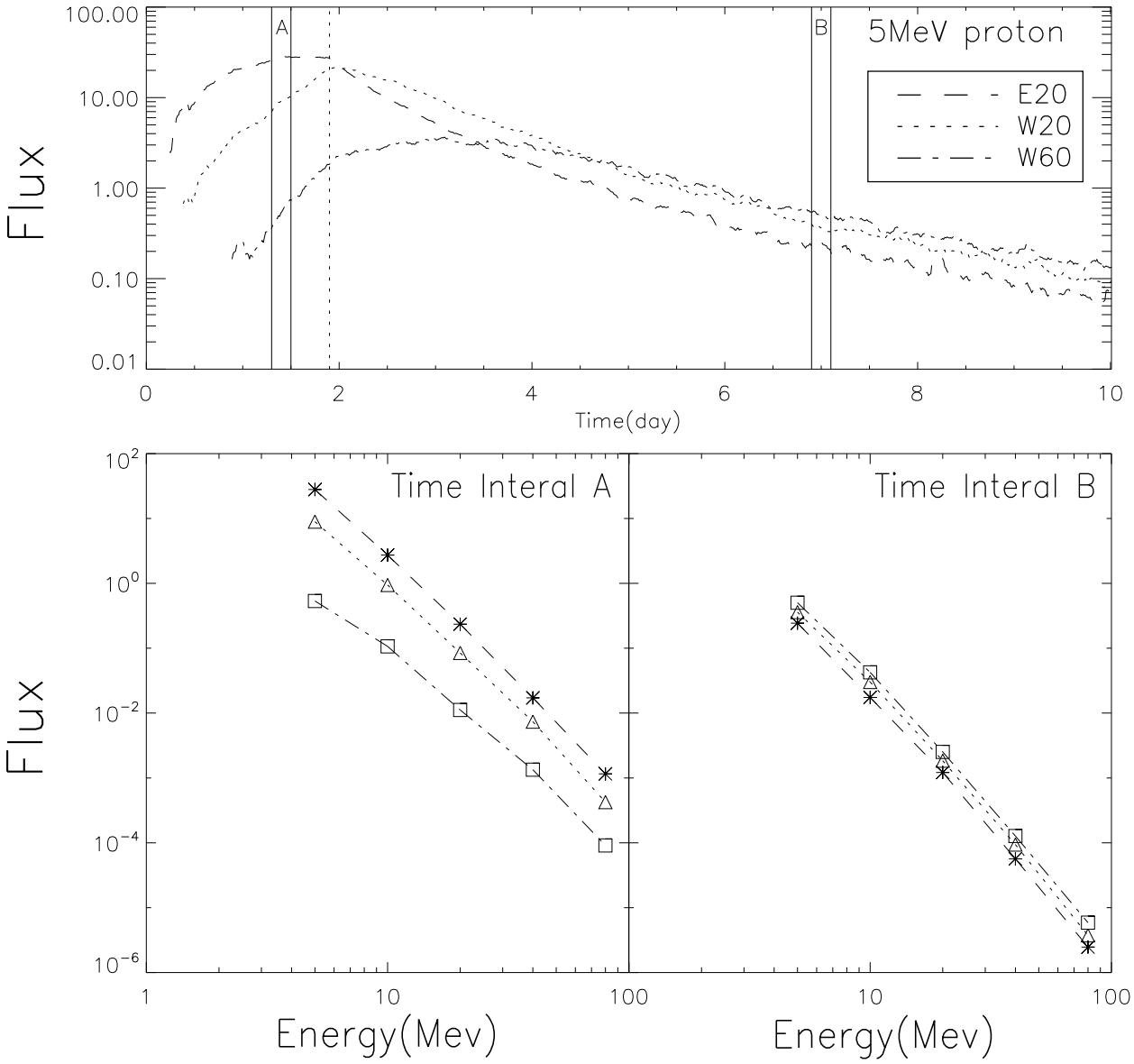

Fig. 3.— In the upper panel, comparison of 5 MeV protons flux observed by the observers in 1 AU ecliptic at different longitudes. The lower left and right panels show the spectra observed at different longitudes during time interval *A* and *B*, respectively. The vertical dashed lines indicate the shock passage of 1 AU.

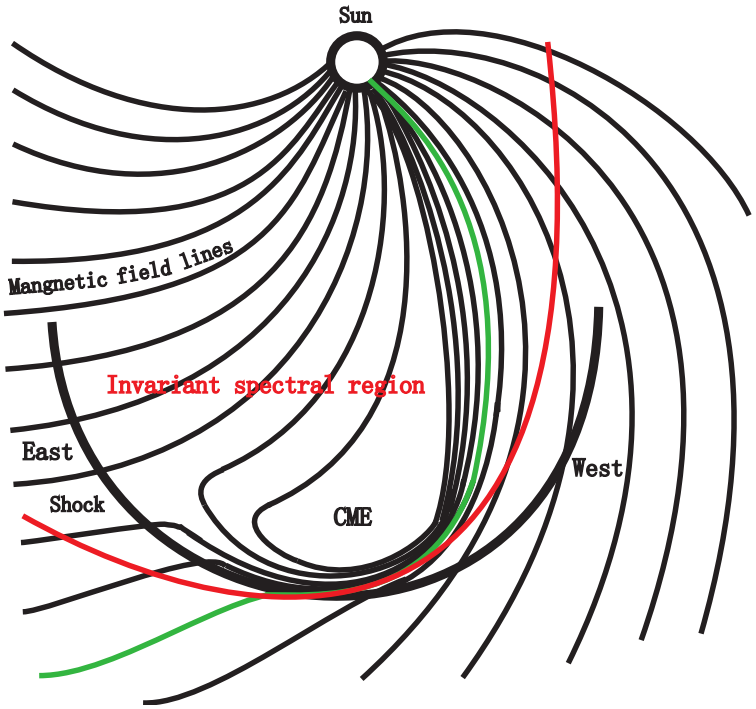

Fig. 4.— The green line indicates the original spectra invariant region proposed by Reames et al. (1997). The red line indicates a new spectra invariant region based on the simulation results in this paper.

Table 1: Model Parameters Used in the Calculations.

Parameter	Physical meaning	Value
V^{sw}	solar wind speed	400 km/s
v_s	shock speed	870 km/s
ϕ_s	shock width	60°
α	shock strength parameter	2[a]
ϕ_c	shock strength parameter	15°[b]
γ	injection spectrum	5.5
B_e	magnetic field strength at the Earth	5 nT
$\lambda_{\parallel}$	particle radial mean free path	0.2 AU[c]
$\kappa_{\perp}$	perpendicular diffusion coeffient	$0.1 \times \kappa_{\parallel}$[d]
r_{b0}	inner boundary	0.05 AU
r_{b1}	outer boundary	50 AU

[a] for 5 MeV protons.

[b] for 5 MeV protons.

[c] for 5 MeV protons in the ecliptic at 1 AU.

[d] for 5 MeV protons in the ecliptic at 1 AU.